# Solute Exchange in Synperonic Surfactant Micelles

**ARTICLE** *in* LANGMUIR · JANUARY 2003

Impact Factor: 4.46 · DOI: 10.1021/la020221d · Source: OAI



**5 AUTHORS**, INCLUDING:

Yahya Rharbi
French National Centre for Scientific Research
**60** PUBLICATIONS **1,087** CITATIONS
SEE PROFILE

Katharina Landfester
Max Planck Institute for Polymer Research
**597** PUBLICATIONS **14,083** CITATIONS
SEE PROFILE

# *Articles*

## Solute Exchange in Synperonic Surfactant Micelles

Yahya Rharbi,[†] Nina Bechthold,[†,‡] Katharina Landfester,[‡] Alex Salzman,[†] and Mitchell A. Winnik*,[†]

*Department of Chemistry, University of Toronto, 80 Saint George Street, Toronto, Ontario, Canada M5S 3H6, and Max Planck Institute of Colloids and Interfaces, Research Campus Golm, 14424 Golm, Germany*

*Received March 5, 2002. In Final Form: September 10, 2002*

We describe experiments that examine the rates of solute exchange in micelles formed from the surfactants Synperonic A7 and Synperonic A50. These surfactants are linear alkane (mixed $C_{13}$ and $C_{15}$) ethoxylates with mean degrees of ethoxylation of 6.5 for A7 and 53.7 for A50. The solute is gycerol-1,2-distearate-3-pyrenebutyrate, **1**. Solutions containing on average 0.4 molecules of **1** per micelle show both excimer and monomer fluorescence. Excimer emission originates from micelles containing at least two pyrene chromophores. In A50, **1** forms aggregates that do not exchange on a time scale of weeks. When solutions of A7 are treated with an excess of empty micelles, the excimer fluorescence decays with a pseudo-first-order rate that depends on the concentration of empty micelles. Because **1** is so insoluble in water, its exchange involves either fusion of two micelles to form a short-lived supermicelle, or fragmentation of a micelle into submicelles, which then grow back to form normal micelles. The corresponding rate constants are $k_2 = 8.7 \times 10^4\ M^{-1}s^{-1}$ for the second-order process and $k_1 = 0.85\ s^{-1}$ for the first-order process. These rates are more than an order of magnitude slower than the rates of micelle fusion and fragmentation for Triton-X100 micelles (Rharbi et al. *J. Am. Chem. Soc.* **2000**, 122, 6242) determined by the same technique. We discuss possible sources for these differences.

### Introduction

Most of our knowledge about micelle dynamics comes from chemical relaxation experiments.[1] In these experiments the system is rapidly perturbed to a nonequilibrium state by changing the temperature, pressure, or surfactant concentration. The relaxation to equilibrium is monitored through the observation of the conductivity if the system is ionic, or by light scattering, circular dichroism, or fluorescence if the micelles are nonionic. These measurements frequently identify two well-separated relaxation times, a rapid relaxation $\tau_1$ that occurs on a time scale of microseconds and a slower process $\tau_2$, which requires milliseconds to seconds or longer. Aniansson and Wall[2] (AW) assigned the fast process to an association-dissociation process involving the exchange of individual surfactant molecules between the micelles and the water phase. This results in change in micelle size without affecting their number. They showed that one could calculate the exit $k^-$ and reentry $k^+$ rate constants for the surfactant molecules from the concentration dependence of the fast relaxation time.

AW attributed the slow process to the reestablishment of equilibrium through cooperative condensation or dissolution of surfactant monomers. These processes result in the creation and breakdown of entire micelles. This process yields a change of both the micellar size and the number of micelles present in solution. These two processes can be represented by the expression

$$S_i + S \rightleftarrows S_{i+1} \tag{1}$$

where $i$ is the number of surfactant molecules S in an aggregate. The AW mechanism excludes reactions between aggregates. Only reactions involving aggregates and free surfactant molecules are allowed.

Two other slow relaxation processes have been suggested in the literature.[3−5] One process involves the fusion of two micelles to form a transient "supermicelle," which subsequently fragments back to two normal micelles. The second process involves the fragmentation of a normal micelle into two short-lived "submicelles," which grow back to normal micelles through fusion or through condensation of free surfactant monomers present in the solution. Fusion and fission processes can be represented by the expression

$$S_i + S_j \rightleftarrows S_{i+j} \tag{2}$$

While relaxation experiments are a powerful means of determining the rates of various relaxation process, it is

[†] University of Toronto.

[‡] Max Planck Institute of Colloids and Interfaces.

(1) For reviews of dynamic processes in micelles, see: (a) Muller, N. in *Solution Chemistry of Surfactants*; Mittal, K. L., Ed.; Plenum: New York, 1979; Vol 1, pp 267−295. (b) Gormally, J.; Gettins, W. J.; Wyn-Jones, E. In *Molecular Interactions*; Wiley: New York, 1980; Vol. 2, pp 143−177. (c) Lang, J.; Zana, R. In *Surfactant Solutions: New Methods of Investigation*; Zana, R., Ed.; Marcel Dekker: New York, 1987; pp 405−452. (d) Huibers, P. D. T.; Oh, S. G.; Shah, D. O. In *Surfactants in Solution*; Chattopadhay, A. K.; Mittal, K. L., Eds.; Marcel Dekker: New York, 1995; Vol. 64, pp 105−121.

(2) (a) Aniansson, E. A. G.; Wall, S. N. *J. Phys. Chem.* **1974**, *78*, 1024; **1975**, *75*, 857. (b) Aniansson, E. A. G.; Wall, S. N.; Almgren, M.; Hoffmann, H.; Kielmann, H.; Ulbricht, W.; Zana, R.; Lang, J.; Tondre, C. *J. Phys. Chem.* **1976**, *80*, 905.

(3) Zana, R. In *Surfactants in Solution*; Mittal, K. L., Bothorel, P., Eds; Plenum Press: New York, 1986; Vol. 4.

(4) Kahlweit, M. In *Physics of Amphiphiles, Micelles, Vesicles, and Microemulsions*; Degiorgio, V., Corti, M., Eds.; North-Holland: Amsterdam, 1985.

(5) Kahlweit, M. *J. Colloid Interface Sci.* **1982**, *90*, 92.

10.1021/la020221d CCC: $25.00 
Published on Web 12/04/2002

difficult, with these data alone, to establish the mechanism associated with each rate. It is particularly difficult to establish the mechanism of the slow process. Herrmann and Kahlweit,[6] for example, carried out extensive pressure-jump and temperature jump measurements on aqueous solutions of Triton ×100 (TX100) micelles. They found that the surfactant-concentration dependence of the slow relaxation rate was inconsistent with the AW mechanism. Alternative explanations include fragmentation and fusion of the micellar species present in the solution. Until recently, there have been no techniques, which allow one to observe and distinguish fusion and fragmentation processes of surfactant micelles.

We recently discovered that solute exchange measurements, using pyrene probes with low water solubility, can be employed to follow the rates of micelle fusion and fragmentation.[7−9] Traditional solute exchange experiments, based on fluorescence quenching or phosphorescence quenching, monitor processes that occur on the time scale of microseconds to milliseconds.[10] This type of exchange normally involves exit of the solute from the micelle into the water phase, diffusion through the water, and entry into a different micelle. To be able to monitor solute exchange that occurs via a collision of two micelles or fragmentation of a micelle into two submicelles, it is necessary to choose a solute that is too insoluble in water for the exit−reentry pathway to be important.

This type of experiment is possible if one employs a pyrene derivative with a strongly hydrophobic substituent. Upon excitation, pyrene derivatives emit a blue structured "monomer" fluorescence in micelles that contain only a single probe. In micelles that contain two (or more) probe molecules, pyrene excimer contributes a broad green emission. A particularly interesting probe is the triglyceride **1**, which has a negligible solubility in water. While one might imagine that a molecule of this size might perturb the properties of a typical surfactant micelle, detailed studies of **1** in Triton X-100 (TX100) show that **1** behaves as a typical pyrene probe.[11a] Like pyrene itself or ethylpyrene, **1** is characterized by a Poisson distribution in aqueous solutions of nonionic micelles. From fluorescence decay studies of these solutions, one recovers the molar concentration of micelles in the solution, from which one can calculate the mean aggregation number $N_{agg}$ of the micelles. For TX100, these studies give a value of $N_{agg}$ of 110 at 24.6 °C, comparable to the number determined by light scattering.[11b]

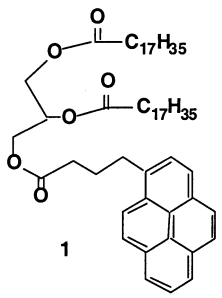


**1**

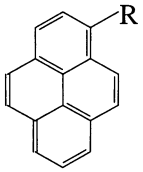


Py-$C_8$, R = n-octyl
Py-$C_{12}$, R = n-dodectyl

In the experiments reported here, we examine **1** as a probe of micelle fusion and fragmentation for the nonionic surfactants Synperonic A7 and Synperonic A50. According to the literature,[12] these surfactants are prepared by the ethoxylation of the natural product Synperol, and the hydrophobe consists of a mixture of 66% linear $C_{13}$ chains and 34% linear $C_{15}$ chains. The ethoxylation process gives rise to a wide distribution of ethoxylated chain lengths ($EO_y$) with an average of $y = 7$ for A7 and $y = 50$ for A50. However, 4.5% of Synperol remains unethoxylated and in A7, 16.5% of the surfactant molecules contain more than 15 EO units. We compare these results with those of experiments carried out with *n*-octylpyrene (Py-$C_8$) and n-dodecylpyrene (Py-$C_{12}$) as fluorescent probes.

## Experimental Section

**Materials.** The nonionic surfactants Synperonic A7 and A50 ($(CH_3\text{-}(CH_2)_x\text{-}CH_2\text{-}(OCH_2\text{-}CH_2)_y\text{-}OH$) were supplied by ICI Americas Inc., Wilmington, Delaware and were used as received. In our laboratory, Li et al.[13] carried out $^1$H NMR measurements at 400 MHz on solutions of these surfactant in $CDCl_3$. They found $x = 8$, $y = 6.5$ for A7 and $x = 9.2$, $y = 53.7$ for A50. The molecule **1** ($M_w = 882$) is a triglyceride in which 4-(1-pyrene)-butyric acid is one of the constituent fatty acid esters. Its synthesis and characterization is described elsewhere,[11a] as are the syntheses and characterization of 1-octyl pyrene and 1-dodecyl pyrene. Distilled water was further purified through a Millipore Milli-Q purification system.

**Surfactant Solutions Containing Pyrene Derivatives.** Individual solution of Synperonic A7 and A50 (34 mM) were mixed with 0.1 mg of each of the pyrene-derivatives. These mixtures were heated at 75 °C and strongly agitated for 15 min with a Vortex Genie 2 model G 560 mechanical shaker at its maximum frequency (>10 Hz). The solutions were then allowed to cool to room temperature over 2 h and then filtered through a 0.2 $\mu$m filter in order to remove a tiny amount of solid. This transparent solution was diluted with aqueous surfactant solution and then with water.

The amount of Py-R solubilized in each synperonic solution was determined by UV spectroscopy using the extinction $\epsilon_{346}$ values of ethylpyrene ($4.3 \times 10^4$ $M^{-1}$ $cm^{-1}$ in A7 and $3.16 \times 10^4$ $M^{-1}$ $cm^{-1}$ in A50) determined previously.[11] Absorption spectra of **1** were measured with a Hewlett-Packard 8452A diode-array spectrometer, using a 1.00 cm cell. The background was subtracted using A7 or A50 solutions of the same concentration as a reference. The absorbance of each of pyrene derivative was calculated relative to that at 398 nm, which was considered as the base line.

**Fluorescence Measurements.** Steady-state fluorescence measurements were carried out with a SPEX (2.1.2) Fluorolog spectrometer in the S/R mode. The intensity was kept below $2 \times 10^6$ counts/s to maintain the linearity of the detector response. For emission spectra and for time-scan kinetics experiments, $\lambda_{ex} = 346$ nm, whereas excitation spectra were obtained for both $\lambda_{em} = 375$ nm (monomer) and $\lambda_{em} = 480$ nm (excimer). The excimer $I_E$ and monomer $I_M$ intensities used in the calculation of $I_E/I_M$ ratio were calculated by integration of emission spectra between 360 and 380 nm for the monomer and 450 to 550 nm for the excimer band.

**Kinetics Experiments.** In kinetics measurements, the samples were mixed in the sample chamber of the fluorescence spectrometer using a home-built stopped-flow injector[9] with a dead time of 2 ms. In each injection, 0.35 mL of a solution containing Py-R in the range of 2.5 $\mu$M **1** + Synperonic A7 (1.0 mM) was mixed with 0.35 mL of pure A7 solution ([A7] varying from 0 to 30 mM). The signal was monitored at either $\lambda_{em} = 375$ nm or $\lambda_{em} = 480$ nm, with integration and interval times of 1 to 10 ms and a total experiment time ranging from 2 to 5 s depending

(6) Herrmann, C.-U.; Kahlweit, M. *J. Phys. Chem.* **1980**, *84*, 1536.
(7) Rharbi, Y.; Winnik, M. A. *Adv. Colloid Interface Sci.* **2001**, *89*, 25.
(8) Rharbi, Y.; Winnik, M. A.; Hahn, K. G. *Langmuir* **1999**, *15*, 4697.
(9) Rharbi, Y.; Li, M.; Winnik, M. A.; Hahn, K. G. *J. Am. Chem. Soc.* **2000**, *122*, 6242.
(10) Almgren, M.; Grieser, F.; Thomas, J. K. *J. Am. Chem. Soc.* **1979**, *101*, 2021.
(11) (a) Rharbi, Y.; Kitaev, V.; Winnik, M. A.; Hahn, K. G. *Langmuir* **1999**, *15*, 2259. (b) Brown, W.; Rymden, R.; van Stam, J.; Almgren, M.; Svensk, G. *J. Phys. Chem.* **1989**, *93*, 2512.
(12) Dimitrova, G. T.; Tadros, Th. F.; Luckham, P. F. *Langmuir* **1995**, *11*, 1101.
(13) (a) Li, M.; Rharbi, Y.; Winnik, M. A.; Hahn, K. G. *J. Colloid Interface. Sci.* **2001**, *240*, 284. (b) $N_{agg}$ values of A7 determined by means of ethylpyrene are 252 at 2.0 g/L, 306 at 5.0 g/L, and 322 at 10 g/L. (c) There is an error in the labeling of the *y*-axis of Figure 3 in ref 13a.

on the decay time. Experiments were carried out at 24.2 ± 0.1 °C. Each experiment was repeated 8 times, and the lifetimes of the individual decays from these runs were averaged.

## Results and Discussion

**Characterization of Aqueous A50 and A7 Solutions.** Recently Li et al.[13] investigated aqueous solutions of Synperonic A7 and A50 by means of dynamic (DLS) and static light scattering (SLS) as well as by fluorescence probe techniques using 1-ethylpyrene as the probe. UV−vis and steady-state fluorescence experiments showed that aqueous A7 and A50 solutions can solubilize pyrene and ethylpyrene. The results of fluorescence decay measurements on these solutions were consistent with a Poisson distribution of the probe molecules among the micelles up to a mean occupancy number $\langle n \rangle = 1$. Analysis of these fluorescence decays in terms of the Poisson quenching model[14] yielded an aggregation number $N_{agg}$ of 300 for A7 and 40 for A50. That study found that $N_{agg}$ values for freshly prepared samples of A7 increase modestly with increasing surfactant concentration.[13b] While the A50 micelles were stable, the A7 micelles grow over a period of a month to $N_{agg} = 700$. Quasielastic light scattering experiments gave a hydrodynamic radius of 3.4 nm for A50 and 5.5 nm for A7, and diffusion coefficients of $2.2 \times 10^{-7}$ cm$^2$/s for A50 and $1.4 \times 10^{-7}$ cm$^2$/s for A7.[13c] The large aggregation number for micelles of A7 make it unlikely that these micelles are spherical in shape.[15] We assume that they are ellipsoidal.

The rate of excimer formation was found to be 2.5 $\mu s^{-1}$ for A7 and 12.5 $\mu s^{-1}$ for A50, which indicates that the core of these micelles is a fluidlike medium. The critical micelle concentrations (cmc) were found to be 0.22 mM for A7 and 0.07 mM for A50.

*Solutions of A50 Containing **1**.* To dissolve **1** in an aqueous solution of A50, crystals of 1 were heated with a solution of the surfactant under vigorous shaking at 75 °C. These solutions were hazy and thus above their cloud point. After cooling to room temperature, the solution was passed through a fine filter to remove any undissolved probe. In Figure 1 we show the emission spectrum of an aqueous A50 solution (1.9 mM) containing 2.3 $\mu$M of **1**. This spectrum exhibits a significant excimer emission at 480 nm in addition to the monomer emission between 360 and 380 nm.

In a well-behaved system, where micelle dynamics maintain the probe with a Poisson distribution among micelles, the excimer intensity will decay to zero in the presence of a vast excess of empty micelles. For a system at equilibrium, the excimer-to-monomer intensity ratio $I_E/I_M$ is predicted to be proportional to the mole ratio of probe-to-micelles.[16]

$$I_E/I_M \sim \langle n \rangle = [\text{Py-R}]/[\text{micelle}] \quad (3)$$

$$[\text{micelle}] = ([\text{surfactant}] - \text{cmc})/N_{agg} \quad (4)$$

This is not the case for **1** in A50, where $I_E/I_M$ remains constant after successive dilutions with pure A50 solution (Figure 2). The signature of a pyrene probe not dissolved as individual molecules within a micelle is an excimer excitation spectrum red shifted from that of the monomer emission.[17] For solutions of **1** in A50, the excitation spectra for the excimer emission ($\lambda_{ex} = 480$ nm) is red-shifted by 2 nm from the excitation spectrum for the monomer emission ($\lambda_{ex} = 375$ nm) as shown in Figure 3. This difference suggests that aggregates of **1** are present, surrounded by A50 molecules, and that the solution also contains empty micelles and micelles containing single molecules of **1**. We could imagine that small micelles, with 25 to 40 surfactant monomers per micelle, do not afford the proper environment to solubilize molecules as large as **1** and maintain a Poisson distribution of solutes.

The emission spectrum of **1** in A50 remains unchanged for more than a month following dilution with a pure A50 solution. This result establishes that the pyrene aggregates in the system do not break down and repartition over this time scale. We have seen a similar behavior when we tried to dissolve **1** directly in aqueous solutions of sodium dodecyl sulfate (SDS). We were able to obtain a solution of free molecules of **1** in SDS only through an

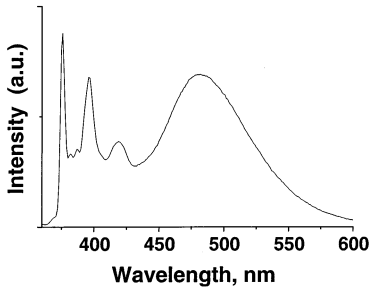


**Figure 1.** Emission spectrum of **1** (2.3 $\mu$M) in aqueous Synperonic A50 solution (1.9 mM). The excitation wavelength was $\lambda_{ex} = 346$ nm.

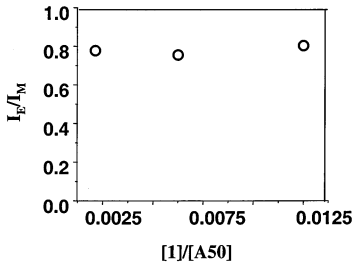


**Figure 2.** The ratio of the monomer to excimer intensities $I_E/I_M$ calculated from the emission spectra of **1** in A50 (1.9 mM) plotted against the mole ratio of **1** to A50. $I_E$ and $I_M$ were calculated by the integration of the emission spectra between 360 and 380 nm for $I_M$ and 450 and 550 for $I_E$.

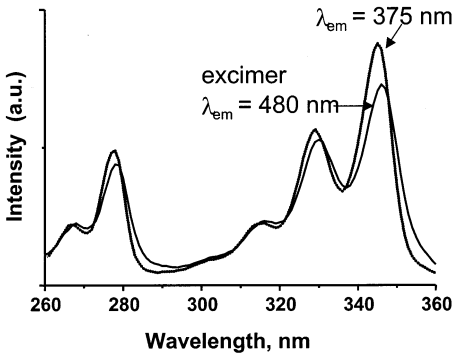


**Figure 3.** Excitation spectrum of **1** (2.3 $\mu$M) in aqueous Synperonic A50 solution (1.9 mM) with $\lambda_{em} = 375$ nm (monomer) compared to the spectrum with $\lambda_{em} = 480$ nm (excimer).

(14) (a) Yekta, A.; Aikawa, M.; Brown, W.; Turro, N. *J. Chem. Phys. Lett.* **1979**, *63*, 543−548. (b) Tachiya, M. *Chem. Phys. Lett.* **1975**, *33*, 289−292. (C) Infelta, P. P.; Grätzel, M.; Thomas, J. K. *J. Phys. Chem.* **1974**, *78*, 190.

(15) Israelachvili, J. *Intermolecular and Surface Forces*, 2nd ed.; Academic Press: San Diego, 1992.

(16) Infelta, P. P.; Grätzel, M. *J. Chem. Phys.* **1979**, *70*, 179.

(17) Winnik, F. *Chem. Rev.* **1993**, *93*, 587−614.

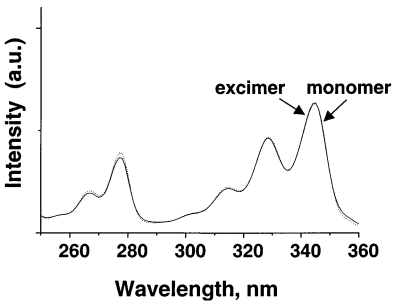


**Figure 4.** Excitation spectrum of **1** (18 $\mu$M) in aqueous Synperonic A7 solution (11 mM) with $\lambda_{em} = 375$ nm (monomer) compared to the spectrum with $\lambda_{em} = 480$ nm (excimer).

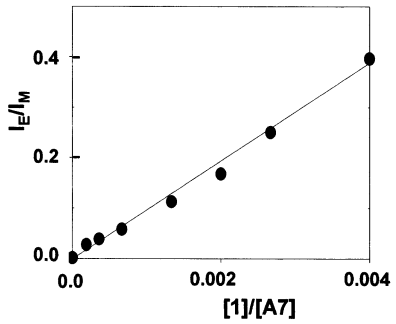


**Figure 5.** The ratio of the excimer-to-monomer intensities $I_E/I_M$ vs the mole ratio of **1** to A7. $I_E/I_M$ was calculated from the emission spectra of **1** in A7 (11 mM) diluted with a pure A7 solution (11 mM).

indirect method, based on experiments on mixed micelles described by Dubin et al.,[18] in which a solution of **1** in TX100 was treated with a large excess of SDS micelles.[19]

*Solutions of A7 Containing Pyrene Derivatives.* The emission spectrum of **1** in aqueous A7 solution ([A7] = 11 mM and [**1**] = 18 $\mu$M) has a broad excimer emission with a peak at 480 nm, in addition to the monomer fluorescence with a (0,0) band at 375 nm. In Figure 4 we show that the excitation spectra of this solution monitored at the emission wavelength of the monomer (375 nm) and that of the excimer (480 nm) superimpose. These spectra have essentially identical features with the monomer excitation spectrum of **1** in tetrahydrofuran solution. These observations suggest the absence of aggregates of **1** in the micelles of A7. When this solution is mixed with A7 solution free of **1**, the excimer peak decreases and the monomer peak increases. After the solutions reach equilibrium, the $I_E/I_M$ is found to be proportional to the number of **1** per micelle (Figure 5), which suggests a Poisson distribution of **1** among the micelles. We also found A7 to be even more efficient in dissolving the probes Py-C12 and Py-C8. From the dependence of $I_E/I_M$ on probe concentration and the excitation spectra of these solutions, we conclude that Py-R derivatives partition to satisfy a Poisson distribution among the micelles up to a mean occupancy number of 1.0.

**Solute Exchange Mechanisms.** Chart 1 illustrates three different mechanisms for the exchange of solutes between micelles. The first mechanism (exit−reentry) involves the exit of the solute from a micelle into water, diffusion through the water phase and then entry into an empty micelle. The second mechanism (collision-exchange-separation) involves four steps: (1) collision of a probe-containing micelle and an empty micelle, (2) formation of

**Chart 1. (A) Exit−Reentry Mechanism. (B) Collision−Exchange−Separation Mechanism. (C) Fragmentation−Growth Mechanism**

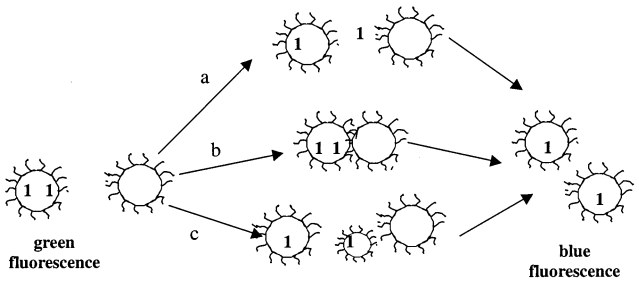


an aggregate consisting of two micelles, (3) exchange of the solute **1** within this aggregate, and (4) separation of the aggregate into two normal-size (proper) micelles. The third mechanism (fragmentation−growth) involves fragmentation of a normal micelle into two submicelles each containing a single solute, followed by growth of these submicelles, either by fusion with empty micelles, or by condensation of surfactant monomers.

In any given exchange experiment, processes described by all three mechanisms could occur simultaneously. Since the rates of these processes have different sensitivities to the surfactant concentration, their individual contributions can be separated. For example, the exit−reentry mechanism and the fragmentation-growth mechanism are characterized by first-order kinetics, whereas the collision-exchange-separation mechanism should exhibit second-order kinetics with a second-order rate constant $k_2$ and a pseudo-first-order exchange rate $k_{obs}$ dependent on the concentration of empty micelles.

Tachiya and co-workers [20] have recently developed a detailed theoretical model to describe the kinetics of solute exchange by the mechanisms shown in Chart 1. In their model they treat explicitly the changes in monomer and excimer fluorescence intensity that accompany the exchange of pyrene-type solutes, including the case in which some micelles contain more than two solutes. In this case, more than one exchange step is necessary for disappearance of the excimer emission.

While these authors[20] have shown that it is possible to analyze exchange data in systems in which some micelles contain more than two probes, the data analysis is more complicated than in the limiting case where micelles contain at most two solutes. In our experiments, we prepared solutions with an initial mean occupancy of 0.4 probes per micelle ($\langle n \rangle = 0.4$). In these solutions, 60% of the micelles contain no probe, 30% of the micelles contain a single probe, and 10% contain two probes. The doubly occupied micelles provide the excimer emission we monitor in our experiments. A negligible fraction of micelles contain three or more probes. When this solution is mixed with an excess of empty micelles, the fraction of micelles $P(t)$ bearing a pair of Py-R should decrease exponentially with time, with a rate characterized by a pseudo-first-order rate constant $k_{obs}$, which contains contributions from all three exchange processes.

$$I_E \propto P(t) = P(0) \exp(-k_{obs}t) \quad (5)$$

$$k_{obs} = k_{exit} + k_1 + k_2[\text{micelle}] \quad (6)$$

Here $k_{exit}$ describes the exit rate of the solute from the micelles, $k_1$ describes the fragmentation rate, and $k_2$

(18) Dubin, P. L.; Principi, B. A.; Smith, M. A.; Fallon, *J. Colloid Interfac. Sci.* **1989**, *127*, 558.
(19) Rharbi, Y.; Winnik, M. A. *J. Am. Chem. Soc.* **2002**, *124*, 2082.
(20) Hilczer, M.; Barzykin, A. V.; Tachiya, M. *Langmuir* **2001**, *14*, 4196.

describes the collision−exchange−fragmentation rate. For a given micelle containing two probes, a single event of fragmentation or collision−fragmentation could have two outcomes. Both probes may remain in one micelle, leaving the other one empty; or each probe could occupy one of the micelles. Only the second process can be observed in our experiment. As a consequence, the true collision−exchange−fragmentation rate constant $k_{fu}$ is twice the experimental values of $k_2$. For the fragmentation process, the interpretation of $k_1$ is more subtle. As we will describe in more detail below, fragmentation can occur in many different ways, and fragments that are too small will be unable to carry a solute molecule. Thus $k_1$ is a lower bound to the overall fragmentation rate.

If one carries out exchange measurements with a probe such as **1** that is effectively insoluble in water, the exit−reentry mechanism is suppressed ($k_{exit} = 0$). Any first-order contribution to the exchange rate must occur by the micelle fragmentation pathway.

$$k_{obs} = k_1 + k_2([\text{surfactant}] - \text{cmc})/N_{agg} \qquad (7)$$

**Exchange Process in A50 and A7.** *Exchange in A50.* Since our method of sample preparation is not effective in providing a solution with molecules of **1** dissolved molecularly in A50 micelles, we cannot draw firm conclusions about the exchange mechanisms that occur in micelles of this surfactant. When mixing a solution of A50 containing **1** with solution of A50 free of probe, no change in the fluorescence spectrum is seen over a period of a month. This is strong indication that the exchange of **1** in A50 micelles is characterized by a rate smaller than $10^{-7}$ s$^{-1}$. There are two possible explanations for this result. The first (and less interesting) explanation is that the time scale of the exchange is determined by the rate of dissociation of the preformed aggregates of **1** in solution. The second explanation is that the $EO_{50}$ chains of the surfactant provide such a substantial steric barrier[21] to core contact between micelle pairs that this second-order exchange process does not occur over a 30 day period.

When studying the exchange of **1** in sodium dodecyl sulfate (SDS) micelles we found extremely slow exchange kinetics with a rate on the order of $10^{-6}$ s$^{-1}$ in the absence of added salt.[19] This exchange occurred almost exclusively by a first-order process. Thus the second-order process, in this range of salt and surfactant concentrations, was substantially slower. In the case of SDS, long-range electrostatic repulsion acts as an efficient barrier preventing collision and fusion of the micelles.[19,22] The fragmentation rate was also suppressed at low ionic strength, and occurred at a rate that increased with the sodium (counterion) concentration as [$Na^+$].[4] For solutions of ionic micelles, the presence of salt has a profound effect on the interaction between headgroups that has no parallel for nonionic micelles.

*Exchange in A7.* In Figure 6, we present the fluorescence spectrum of **1** in an aqueous solution of A7 ([A7] = 2.25 mM, [**1**] = 3.7 $\mu$M). The spectrum labeled "Prior" has a broad excimer emission with a peak at 480 nm in addition to the monomer fluorescence with a (0,0) band at 375 nm. When mixed with a concentrated solution of A7, the spectrum evolves within few seconds to that labeled "after exchange." This spectrum has a strong monomer emission, but no discernible excimer band. In Figure 7 we show the exchange experiment in which we monitor the increase

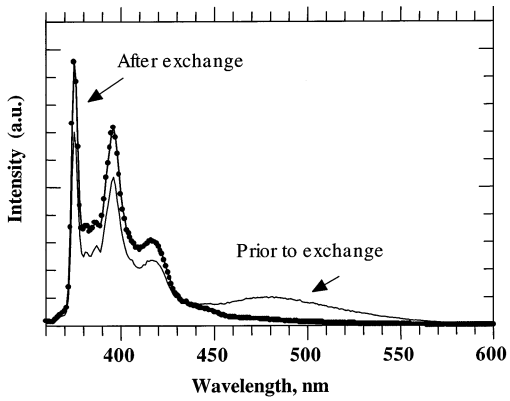


**Figure 6.** Emission spectra ($\lambda_{ex}$ = 346 nm) of **1** solubilized in aqueous solution of A7 micelles. In the spectrum labeled "Prior to exchange," [**1**] = 3.7 $\mu$M and [A7] = 2.25 mM. The spectrum "After exchange" refers to the solution obtained by mixing the original solution with an equal volume of A7 solution to raise the surfactant concentration to [A7] = 20 mM.

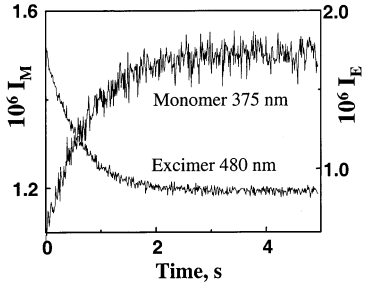


**Figure 7.** Time-scan experiments monitoring the increase in the monomer emission $I_M$ ($\lambda_{em}$ = 375 nm) and the decrease in the excimer emission $I_E$ ($\lambda_{em}$ = 480 nm) after stopped-flow mixing of a solution of **1** in A7 micelles ([**1**] = 3.7 $\mu$M, [A7] = 2.25 mM) with an equal volume of A7 solution ([A7] = 11 mM) at a temperature of 24.2 °C.

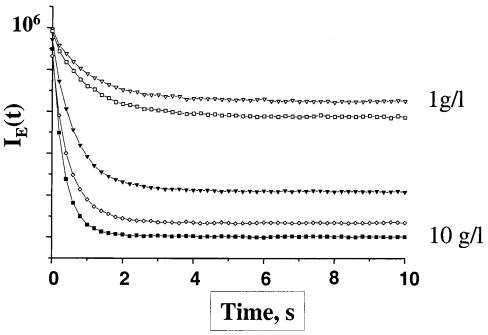


**Figure 8.** Time scan experiments monitoring the decrease of $I_E$ upon stopped flow mixing of a solution of **1** in A7 micelles ([**1**] = 3.7 $\mu$M, [A7] = 2.25 mM) with equal volumes of A7 solutions with [A7] ranging between 2.25 and 22.5 mM.

of $I_M$ and the decrease of $I_E$ upon stopped-flow mixing of aqueous solutions of **1** in A7 with a solution of A7 free of **1** (22 mM). Both the $I_E$ and $I_M$ curves fit to a single-exponential expression with the same decay time. When the kinetics experiments were repeated at different A7 concentrations, we found a strong dependence of $k_{obs}$ on the concentration of unoccupied micelles (Figure 8). The relaxation rates $k_{obs}$ calculated from the fits of the individual decays at 24.2 °C vary between 0.78 and 5 s$^{-1}$.

The dependence of $k_{obs}$ for **1** on the concentration of empty A7 micelles is shown as the bottom line in Figure 9. The concentration of micelles is calculated with eq 4 with $N_{agg}$ = 300 and cmc = 0.22 mM.[13] Values of $k_{obs}$ were calculated by fitting individual $I_E$ decays to an exponential

(21) Halperin, A.; Alexander, S. *Macromolecules* **1989**, *22*, 2403.
(22) Lessner, E.; Teubner, M.; Kahlweit, M. *J. Phys. Chem.* **1981**, *85*, 1529; *J. Phys. Chem.* **1981**, *85*, 3167.

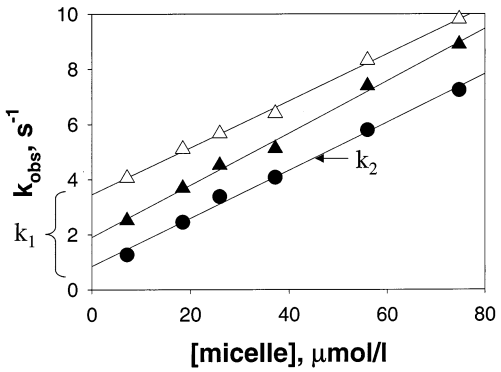


**Figure 9.** The relaxation rates $k_{obs}$ at 24.2 ± 0.1 °C, from fits of the individual $I_E$ decays monitored at $\lambda_{em} = 480$ nm with $\lambda_{ex} = 346$ nm, plotted against the concentration of empty A7 micelles for exchange experiments with three pyrene-derivatives: top, 1-octylpyrene; middle, 1-dodecylpyrene; bottom, **1**.

profile. There are two main features of these plots: 1) an important linear dependence of $k_{obs}$ on the concentration of empty micelles, and 2) a finite intercept, $k_1 = 0.85$ s$^{-1}$. According to eqs 4 and 5, the plot in Figure 9 indicates that there are two distinct mechanisms for solute exchange, a second-order process represented by the linear dependence of $k_{obs}$ on [micelle] competing with a first-order process characterized by the finite intercept.

When these experiments were repeated with the smaller pyrene-derivatives Py-$C_{12}$ and Py-$C_8$ at 24 °C, we also found a linear dependence of $k_{obs}$ on the concentration of empty micelles with slopes parallel to that of **1**, finite intercepts of $k_1 = 1.9$ s$^{-1}$ for Py-$C_{12}$ and 3.4 s$^{-1}$ for Py-$C_8$. These data are shown in the middle and upper traces, respectively, in Figure 9.

*Second-Order Process.* The linear dependence of $k_{obs}$ on [micelle] for **1** is the result of a second-order kinetic process with a rate constant $k_2 = 8.7 \times 10^4$ M$^{-1}$s$^{-1}$. This rate constant is a factor of 20,000 smaller than the diffusion controlled rate constant $k_{diff}$ for collision of two micelles of A7. A value for $k_{diff}$ ($2.3 \times 10^9$ M$^{-1}$ s$^{-1}$ at 24 °C) was calculated with eq 8 (where $N_A$ is Avogadro's number) using previously measured values of the diffusion coefficient $D$ and the hydrodynamic radius $R_H$ of the micelles. The major assumption of this analysis is that the values of $D$ and $R_H$ are not significantly different in the empty micelle ($D_1$ and $R_{H1}$) than when the probe is present ($D_2$ and $R_{H2}$).

$$k_{diff} = 4\pi N_A(R_{H1} + R_{H2})(D_1 + D_2)/1000 \qquad (8)$$

These results establish that the rate of probe exchange is determined by the activation energy for bringing the cores of the two micelles together.

In the second-order mechanism shown in Chart 1, one can imagine two distinct processes for solute exchange between the two micelles. In the fusion mechanism, a transient supermicelle is formed, the probes become randomized in its interior, and then the supermicelle fragments into two normal micelles. In the sticky collision mechanism,[23] the two micelles remain adjacent long enough for the probe to exit one micelle, pass through the interface rich in EO segments, and enter into the adjacent micelle. In our study of the exchange of **1** in TX100 micelles, we argued that passage through the interface would be the rate-limiting step of the sticky-collision mechanism, and the rate of this process would likely depend on the chemical structure of the probe. In A7 we find that three probes undergo second-order exchange at nearly identical rates (Table 1). We conclude that exchange involves complete fusion of the two micelles followed by fragmentation.

(23) Taisne, L.; Cabane, B. *Langmuir* **1998**, *14*, 4744.

**Table 1. Values of the First Order ($k_1$) and Second Order ($k_2$) Rate Constants for Solute Exchange in Micelles of Synperonic A7 and Triton X-100**

| | A7 ($N_{agg} = 300$)[a] | | TX100 ($N_{agg} = 110$)[b] | |
|---|---|---|---|---|
| pyrene-R | $10^{-4}k_2$ (M$^{-1}$ s$^{-1}$) | $k_1$ (s$^{-1}$) | $10^{-4}k_2$ (M$^{-1}$ s$^{-1}$) | $k_1$ (s$^{-1}$) |
| **1** | 8.7 | 0.85 | 150 | 14 |
| Py-$C_{12}$ | 9.4 | 1.9 | 180 | 40 |
| Py-$C_8$ | 8.5 | 3.4 | 200 | 47 |

[a] Experiments carried out at 24.2 °C. [b] Experiments carried out at 24.6 °C.

*First-Order Process.* The first-order exchange process for **1** is characterized by $k_1 = 0.85$ s$^{-1}$. The corresponding value for Py-$C_{12}$ is 1.9 s$^{-1}$; and for Py-$C_8$, 3.4 s$^{-1}$. This exchange can in principle be due either to a fragmentation−growth process or an exit−reentry process. We begin this section with an examination of the hypothesis presented above that the exit−reentry process is too slow to contribute to the rates we observe.

The "exit−reentry" process is controlled by the exit step, with rate constant $k_{exit}$. The entry step is diffusion-controlled with a rate constant $k_{entry}$ ranging from $10^9$ and $10^{10}$ M$^{-1}$s$^{-1}$.[24] The ratio of these rate constants is the partition equilibrium constant for the probe. Its magnitude, like that of $k_{exit}$, depends on the water solubility of the probe. The exit rate can be estimated with the expression

$$k^- = k^+[P]_w/n^* \qquad (9)$$

where $[P]_w$ is the water solubility of the solute, and $n^*$ is the average number of solutes per micelle at the solubility equilibrium. As general rule, both $[P]_w$ and the exit rate of a solute from a micelle decrease by an order of magnitude for every additional two $CH_2$ groups in a series of similar solutes. In more quantitative terms, $[P]_w$ is given by

$$[P]_w = [P]_w^0 \times 10^{-0.6n} \qquad (10)$$

where $n$ is the number of additional $CH_2$ groups, and $[P]_w^0$ is the known water solubility for a derivative with $n = 1$ or 2. Taking the reference value as that of 1-ethylpyrene at 24 °C, for which $[P]_w^0 = 1 \times 10^{-7}$ M, we estimate the exit rates to be on the order of $10^{-22}$ s$^{-1}$ for **1**, $4 \times 10^{-4}$ s$^{-1}$ for Py-$C_{12}$, and $10^{-1}$ s$^{-1}$ for Py-$C_8$. These values are substantially lower than those of the intercepts in Figure 9.[25]

Another estimate of the value of $k_{exit}$ for Py-$C_{12}$ and Py-$C_8$ is provided from our studies of solute exchange in SDS micelles. In this system, the second-order exchange rate was extremely slow, nearly undetectable, for NaCl concentrations less than 100 mM.[19] We inferred that **1** exchanged by a fragmentation-growth mechanism, because added salt strongly accelerated the exchange rate. Py-$C_{12}$ and Py-$C_8$ behaved differently. Their exchange rates decreased when salt was present in the medium. We inferred that Py-$C_{12}$ and Py-$C_8$ exchange by passage of individual solute molecules through the water phase, with

(24) Zana, R. In *Surfactant Solutions: New Method of Investigation*; Zana, R., Ed.; Marcel Dekker: New York, 1987

(25) From eqs 7 and 8, $[P]_w$ was estimated to be on the order of $10^{-32}$ M$^{-1}$ for **1**, $10^{-15}$ M$^{-1}$ for Py-$C_{12}$, and $10^{-11}$ M$^{-1}$ for Py-$C_8$.

**Chart 2**

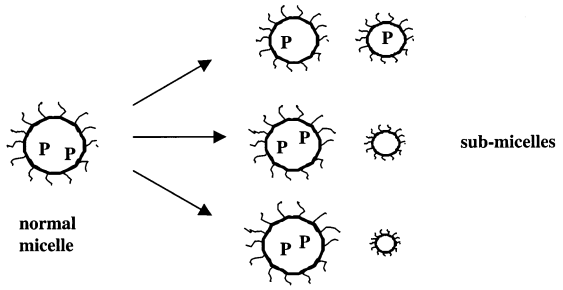


low-salt $k_{exit}$ values of $5 \times 10^{-3}$ $s^{-1}$ for Py-$C_{12}$ and $4 \times 10^{-1}$ $s^{-1}$ for Py-$C_8$. The salt effect is readily understandable from eq 10, since $[P]_w$ decreases in the presence of salt. If the exit rate of a solute is not very sensitive to the nature of the micelle from which it exits, we can take these values as characteristic of the exit rates for Py-$C_{12}$ and Py-$C_8$ from A7 micelles. In all cases $k_1$ is much larger than $k_{exit}$. The first-order exchange rates determined from the intercepts in Figure 9 cannot be due to exit−reentry. They must be due to a fragmentation-growth mechanism.

We next consider what factors may affect the probe-dependence of the experimentally determined micelle fission rate. These first-order rate constants increased as the size of the probe decreased, but the magnitude of the change was relatively small, varying from $k_1 = 0.85$ $s^{-1}$ for **1**, to 3.4 $s^{-1}$ for Py-$C_8$.

The presence of the probe can influence the measured rate of the first order process in two ways. First, micelle fragmentation itself may be intrinsically slower in micelles bearing a probe than in empty micelles. Another factor can contribute to the finding that $k_1$(**1**) < $k_1$(Py-$C_{12}$) < $k_1$(Py-$C_8$). Fragmentation of a large micelle containing $S_f$ surfactant molecules and 2 molecules of probes leads to formation of two submicelles containing $S_i$ and $S_{f-i}$ surfactant molecules, with $i$ varying from 2 to $f-2$. Although fragmentation can produce submicelles of any size, only events resulting in two submicelles sufficiently large to transport a solute can contribute to the exchange rate measured in our experiment. We illustrate this point of view in Chart 2, where P represents a pyrene probe. Other fragmentation events, which produce a submicelle too small to carry a solute molecule, do not contribute to the exchange observed by our experiment, since both Py-R molecules will remain in the larger fragment.

## Conclusions

Time-scan studies of the decay of excimer emission in Synperonic A7 micelles, using pyrene probes of low water solubility, indicate that there are two distinct mechanisms for solute exchange. The process that exhibits second-order kinetics involves collision of two micelles, fusion to form a short-lived supermicelle, and its subsequent fragmentation to two normal micelles. We found identical values of the second-order rate constant ($k_2 = 8.7 \times 10^4$ $M^{-1}$ $s^{-1}$) for the three probes that we examined, **1**, Py-$C_{12}$, and Py-$C_8$. Since the probes themselves have very different structures, we conclude that the fusion rate, which we deduce to be the rate-limiting step, is not sensitive to the presence of the probe in the micelle.

The process that exhibits first order kinetics involves fragmentation of a micelle bearing two probe molecules into two submicelles, each bearing one of the probes. These small structures grow back to normal micelles through condensation of free surfactant monomer or by coalescence with empty submicelles present in the solution. We found that the three probes exhibit first-order rate constants that increased as the size of the probe decreased. The magnitude of the change was relatively small,

**Chart 3**

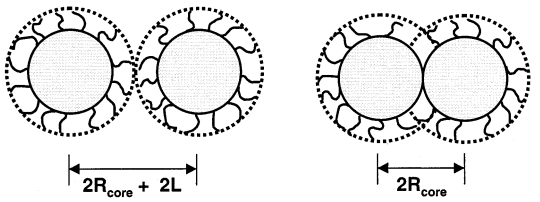


We close this article with a comparison of the exchange rates for **1** in Synperonic A7 micelles with those we reported previously in Triton X-100 micelles. These values are collected in Table 1. The interesting result is that both exchange processes are faster in TX100 micelles. The $k_2$ values are nearly 20 times larger than the values determined here for A7. The $k_1$ values are 10 times larger for TX100 than those for A7.

TX100 forms spherical micelles with an aggregation number of approximately 100 at 25 °C with a narrow size distribution. The micelles are stable over time. A7 forms micelles which are too large to be spherical in shape and are likely ellipsoidal. Their aggregation number, as determined by fluorescence quenching with ethylpyrene as the probe, increases with surfactant concentration. The rate of excimer formation for pyrene derivatives in A7 micelles ($k_Q = 2.5$ $\mu s^{-1}$) is similar to that in TX100 micelles ($k_Q = 3.5$ $\mu s^{-1}$). The magnitude of $k_Q$ is inversely related to the product of the local viscosity (i.e., "microviscosity") of the micelle core times its volume. If we take into consideration difference in the micelle size ($N_{agg}$(TX100) = 100 and $N_{agg}$(A7) = 300), we infer a more fluid like core for A7 micelles than for TX100. If fusion of the micelles were controlled by the fluidity and flexibility of the micelle core, A7 would exhibit a faster fusion process.

Halperin and Alexander (HA),[21] and more recently, Dormidontova,[26] have analyzed the relaxation properties of polymeric micelles. Polymeric micelles are formed from diblock copolymers with an insoluble block of length $N_B$, and a soluble block of length $N_A$. The insoluble block forms a dense liquid core of radius $R_{core}$; the soluble block is anchored at the surface of the core. The corona it forms, of thickness $L$, is swollen by the solvent. HA develop their analysis in the context of three free energy terms that contribute to the structure of the micelles: the free energies per molecule of the core $F_{core}$, the corona $F_{corona}$, and the interface $F_{ifc}$. For a micelle of aggregation number $f$, the corresponding free energies per micelle $\Phi(f) = fF$. To extend their ideas to micelle relaxation processes, they introduce the concept that an intermediate state, for which they can assume a reasonable structure, is useful model of the activated state of the process. Their model for the intermediate state for fusion or fission of consists of two polymeric micelles in close proximity with their cores in grazing contact and the coronas partly overlapping. A drawing of this state for micelles characterized by relatively short stabilizing chains is shown on the right-hand side of Chart 3.

HA assert that the coronal contribution to the activation free energy for fission $\delta\Phi_{fission}$ is negligible compared to $\Phi_{core}$ and $\Phi_{ifc}$. For an aggregate of $f$ molecules fragmenting into two smaller units of $f_1$ and $f_2$ molecules, they write

$$\delta\Phi_{fission} = \Phi(f_1) + \Phi(f_2) - \Phi(f) \qquad (11)$$

(26) Dormidontova, E. E. *Macromolecules* **1999**, *32*, 7630.

where for fission $\Phi(f)$ is given by

$$\Phi(f) = \Phi_{core} + \Phi_{ifc} \quad (12)$$

The changes in $F_{ifc}$ relate to the increase in surface area accompanying the formation of two smaller micelles. For spherical micelles characterized by thin coronas, this contribution to the activation free energy is given by[21]

$$\delta\Phi_{fission}(\text{interface})/k_BT = (4\pi)^{1/3}3^{2/3}R_{core}{}^2(\gamma/k_BT)[x^{2/3} + (1-x)^{2/3} - 1] \quad (13)$$

with $$x = f_1/f$$

where $\gamma$ is the interfacial tension, and $k_BT$ is the product of the Boltzmann constant times the absolute temperature. According to eq 13, the activation energy for fission depends on the surface area of the parent micelle as well as the sizes of the two daughter micelles. The latter term makes the largest contribution to the activation energy for fission that leads to the formation of two equally sized fragments ($f_1 = f/2$).

In polymeric micelles, the change in $F_{core}$ depends on the change in stretching of the insoluble block. It is more difficult to account for changes to $F_{core}$ for simple nonionic micelles such as A7 and TX100, where the changes in $F_{core}$ are related to the free energy costs of obtaining a dense-packed core with a suboptimal number of surfactants per submicelle. Equation 13 predicts that the micelle with the larger core radius (A7) will have the larger activation energy for fission, in accord with our findings.

HA comment that the activation free energy for fusion is due primarily to coronal interactions. For micelles with thin coronas, they compare the intermediate state shown on the right-hand side of Chart 3, where the distance between the centers of the micelles is $2R_{core}$, with the reference state in which the coronas are just touching but not interacting. Here distance between the centers of the micelles is $(2R_{core} + 2L)$. Under these circumstances,

$$\frac{1}{k_BT}\delta\Phi_{fusion} \approx \frac{vf^3}{R_{core}{}^3}N_A{}^2 \quad (14)$$

where $v$ is the second virial coefficient for the corona blocks.

According to eq 14, for polymeric micelles with a similar core, the barrier to fusion will be larger for the micelle with the longer corona chains. At first glance, this prediction appears to be in the opposite direction from our experimental results: If we describe the structure of both surfactants as R-EO$_y$, where R is the hydrophobe, $y$ takes a mean value of 9.6 for TX100 and 6.5 for A7. We do know, however, that there is a much larger distribution of EO chain lengths in A7. According to ref 10, 4.5% of the Synperol remains unethoxylated in A7 and 16.5% of the chains have more than 15 EO units. These longer chains may dominate the steric stabilization of A7 and increase the barrier to fusion.

We conclude that the HA model of block copolymer micelle dynamics provides a useful framework for understanding fusion and fragmentation processes in nonionic micelles.

**Acknowledgment.** The authors thank ICI, ICI Canada, and NSERC Canada for their support of this research.

LA020221D